Since January 2020 Elsevier has created a COVID-19 resource centre with free information in English and Mandarin on the novel coronavirus COVID-19. The COVID-19 resource centre is hosted on Elsevier Connect, the company's public news and information website.

SLAS Discovery 27 (2022) 79–85

Contents lists available at ScienceDirect

SLAS Discovery

journal homepage: www.elsevier.com/locate/slasd

Full Length Article

Discovery of SARS-CoV-2 main protease covalent inhibitors from a DNA-encoded library selection

Rui Ge[a], Zuyuan Shen[a], Jian Yin[a], Wenhua Chen[a], Qi Zhang[a], Yulong An[a], Dewei Tang[a], Alexander L. Satz[b], Wenji Su[a,*], Letian Kuai[c,*]

[a] WuXi AppTec, 288 Fute Zhong Road, Waigaoqiao Free Trade Zone, Shanghai 200131, China
[b] WuXi AppTec, Am Klopferspitz 19a, 82152 Martinsried, Germany
[c] WuXi AppTec· 55 Cambridge Parkway, 8th Floor· Cambridge, MA 02142, USA

ARTICLE INFO

Keywords:
Covalent inhibitor
Covalent DEL selection
SARS-CoV-2 M^{pro}
COVID-19

ABSTRACT

Covalent inhibitors targeting the main protease (M^{pro}, or 3CLpro) of SARS-CoV-2 have shown promise in preclinical investigations. Herein, we report the discovery of two new series of molecules that irreversibly bind to SARS-CoV-2 M^{pro}. These acrylamide containing molecules were discovered using our covalent DNA-encoded library (DEL) screening platform. Following selection against SARS-CoV-2 M^{pro}, off-DNA compounds were synthesized and investigated to determine their inhibitory effects, the nature of their binding, and to generate preliminary structure-activity relationships. LC-MS analysis indicates a 1:1 (covalent) binding stoichiometry between our hit molecules and SARS-CoV-2 M^{pro}. Fluorescent staining assay for covalent binding in the presence of cell lysate suggests reasonable selectivity for SARS-CoV-2 M^{pro}. And lastly, inhibition of enzymatic activity was also observed against a panel of 3CLpro enzymes from different coronavirus strains, with IC_{50} values ranging from inactive to single digit micromolar. Our results indicate that DEL selection is a useful approach for identifying covalent inhibitors of cysteine proteases.

Introduction

The pandemic of coronavirus disease (COVID-19) sweeping across the world has caused huge losses to lives and economies since its outbreak in December 2019. [1–2] Despite the promising efficacy of vaccines in preventing COVID-19 [3–5], developing effective oral drugs for the treatment of coronavirus infections remains urgent. Various strategies have been applied to find small-molecule drugs for the treatment of coronavirus disease including the repurposing of known anti-viral drugs, high-throughput screening campaigns, virtual screening, and AI-facilitated drug design. [6–11]

The main protease (M^{pro}, or 3CLpro) of SARS-CoV-2 virus that causes COVID-19, is one of the potential targets of drug repurposing or de novo design, due to its critical role in coronavirus replication and transcription. [12–14] In addition, M^{pro} is a highly conserved cysteine protease among coronaviruses, but with no analogues in the human proteome in terms of recognition sequence and cleavage site [15], which makes it a promising target for designing small-molecule drug candidates. A series of ketone- or aldehyde-based covalent inhibitors of SARS-CoV-2 M^{pro} that interact with the catalytic Cys145 at the active site of this enzyme have been reported, and crystal structure analysis indicates reversible covalent binding with Cys145 in the main pocket. [16–17] These inhibitors are generally derived from the previous anti-viral drugs, and possesses a peptidic scaffold and aldehyde functional group for reversible covalent binding. Considering the reported mutations of SARS-CoV-2, it is vital to develop alternative scaffolds and new warheads, to overcome possible resistance mutations of the coronaviruses. [18]

With several covalent inhibitors approved for cancer treatment during the past decade, recent interest in covalent drug discovery has spiked. [19–21] However, finding targeted covalent inhibitors (TCI) is still challenging. Collections of molecules containing suitable electrophilic warheads are lacking, and a major risk of high-throughput screening of these low chemical diversity collections is the interference by over-reactive electrophiles. [22–23] An alternative strategy of generating TCIs is to modify known non-covalent ligands or fragments by attaching an electrophilic group that can react with a proximal nucleophilic amino acid, which is usually a cysteine, but can be serine,

Abbreviations: DEL, DNA-encoded library; M^{pro}, main protease; TCI, tar-geted covalent inhibitors; LC-MS, liquid chromatog-raphy/mass spectrometry; BTK, Bruton's tyrosine kinase; JNK1, c-Jun *N*-terminal protein kinase 1; Fmoc, 9-fluorenylmethyloxycarbonyl; PCR, polymerase chain reaction; SDS-PAGE, sodium dodecyl sulphate-polyacrylamide gel electrophoresis.

* Corresponding authors.
E-mail addresses: su_wenji@wuxiapptec.com (W. Su), letian_kuai@wuxiapptec.com (L. Kuai).

https://doi.org/10.1016/j.slasd.2022.01.001

Available online 19 January 2022

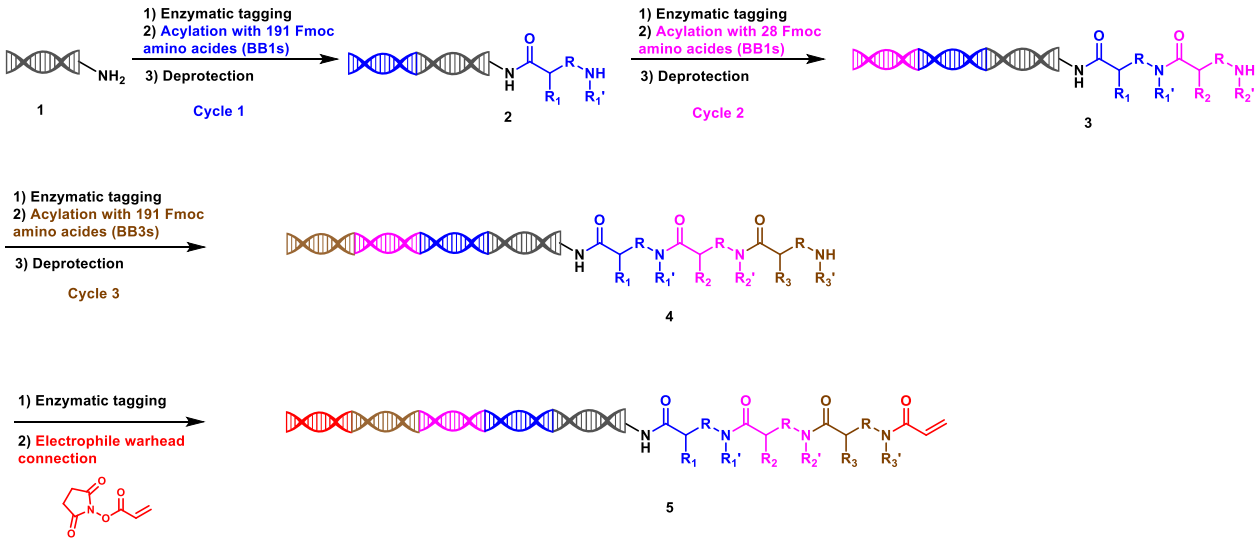

Scheme 1. Synthesis of the covalent DNA Encoded Library 4

tyrosine or a few other amino acids as well. [24–26] However, the pool of known non-covalent ligands to select from is usually not large enough, and the rational design of potent covalent ligands from fragments that bind the target non-covalently can be a daunting task. Therefore, the combination of readily produced DNA-encoded libraries (DEL) of electrophiles coupled with a covalent selection method can provide a promising way to address these limitations and challenges. [27]

DEL is an emerging technology that allows constructing and screening millions to billions of compounds, in a cost-effective and efficient manner. [27–35] Several laboratories have investigated the use of DELs, employing widely varied formats, to discover covalent hit molecules. Chan *et al.* reported the discovery of a covalent inhibitor of MAP2K6 with the 50% inhibitory concentration (IC_{50}) 4.5 μM using a template DEL strategy. [36] Zimmermann *et al.* showed the identification of covalent binders against JNK-1 using an encoded self-assembling chemical library. [37] Zambaldo *et al.* used a DNA library in a microarray format to discover covalent hits against kinases MEK2 and ERBB2. [38] Zhu *et al.* demonstrated the use of an on-DNA tool compound with HRV 3C protease. [39] And perhaps most relevant to our work, Guilinger *et al.* reported a covalent DEL selection to identify Bruton's tyrosine kinase inhibitors. [40] Despite these examples, covalent DEL selection against protein targets remains challenging in a few aspects: 1) the diversity of covalent libraries in terms of electrophiles with different reactivity; 2) the optimal incubation conditions for different protein target and electrophile combinations; and 3) methods of achieving adequate signal-to-noise to identify potential covalent hits from one round of selection, particularly against target classes other than kinases.

In this study, we utilized a self-designed and constructed covalent DEL, in combination with an optimized covalent screening method, to discover novel covalent inhibitors of SARS-CoV-2 M^{pro}. The potential covalent binders were validated through off-DNA compounds synthesis, covalent binding analysis, and functional assay. Our results indicate the feasibility and effectiveness of covalent DEL selection for hit discovery, in particular against viral proteases.

Results and discussion

Covalent DEL Libraries

DNA encoded library technology adopts split-and-pool strategy to generate combinatorial small molecules, each labeled with its unique DNA sequence. Our DNA encoded covalent libraries were designed with three or four cycles of chemistry plus the coupling of electrophiles. After testing the stability of different covalent electrophiles in DNA-compatible reaction conditions, 3 common covalent electrophiles focusing on targeting cysteine were chosen for library construction, to create a complexity of more than 600 million chemical structures. One of library (library 4) is taken as an example (Scheme 1). 191 Fmoc amino acids at cycle-1 (referred to as BB1) were first installed by acylation reaction onto the primary amine on the oligonucleotide headpiece after encoded with 191 unique oligonucleotide tags. After pooling, deprotection of *N*-Fmoc, the cycle-1 product was split into 28 wells, and encoded with 28 oligonucleotide tags prior to installing 28 Fmoc amino acids at cycle-2 (BB2) by acylation reaction. After pooling, deprotection of *N*-Fmoc, and splitting again into different wells, 191 unique Fmoc amino acids at cycle-3 (BB3) were reacted though amide bond formation after encoded with 191 unique oligonucleotide tags. Through pooling, *N*-Fmoc deprotection and encoding with a unique oligonucleotide tag, the electrophiles were then attached to the intermediate libraries by amide bond formation in the last synthetic step. Thus, the same intermediate libraries were reacted with different electrophiles to produce a series of libraries with variable electrophilic warheads. A brief illustration of our covalent DEL libraries are listed in Table S1.

Covalent DEL Selection

A general procedure of covalent DEL selection includes incubation, immobilization, wash and elution. Note that the incubation time, concentrations of the covalent libraries, and the amount of target protein need to be assessed through condition optimization, as the optimal incubation condition might vary from case to case depending on the accessibility of cysteine among different protein targets and the desired hit profile.

Briefly, 3CLpro was incubated with the 10 pmol covalent DEL pool, comprised with 9 libraries with a total of 1.87 billion diversity in Tris-HCl (pH 7.5) buffer at room temperature for 1 hr. The 3CLpro protein was then immobilized on the Ni-NTA beads matrix through *C*-terminal 6xHis-tag. After three rounds of washing steps to remove unbound library members, protein: library-member complexes were eluted from the matrix by addition of 250 mM imidazole 30 min, and size exclusion chromatography purification was performed to remove excessive imidazole from the elution. The purified samples were then subjected to PCR amplification and NGS sequencing, similar to our previously published protocols for DEL selection for reversible ligands. [41] It is worth noting that the competitive elution method does not completely eliminate the presence of non-covalent binders.

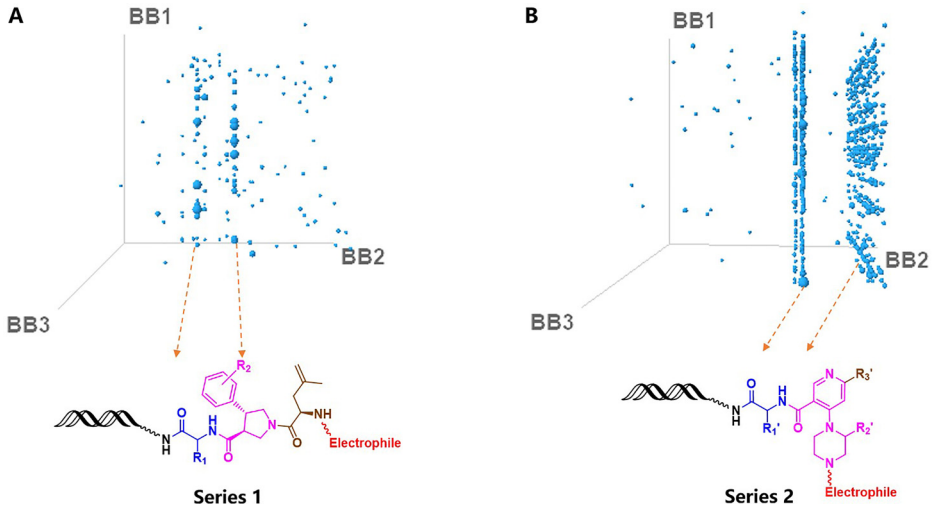

Figure 1. Cubic plot of libraries with preferred scaffolds and the corresponding structural features, where each axis represents one cycle of chemistry, and the size of each dot proportional to the copy counts of a unique compound. (**A**) For series 1, the BB2 and BB3 showed clear structural features with various BB1. (**B**) For series 2, the BB2 showed enriched structural features with aromatic substitution of BB3 and various BB1.

The structure of enriched molecules was decoded through the DNA translation table from the sequencing data set. Further analysis of the affinity selection output was performed using Spotfire and presented in a cube view (Fig. 1). Compounds that were over 5 folds enriched than average are shown with the cube, where each axis represented building blocks used in cycle-1, cycle-2, and cycle-3 chemistry, respectively. Each blue dot represents a unique compound, and the size of each dot is proportional to the copy counts of each compound. Through clustering analysis of building blocks in different cycles, unique structural patterns that represent potential hits can be identified. Features sharing one or more building blocks can be easily recognized in the cube view as lines or planes. [41–42] Analysis of these data revealed several features from two enriched libraries. The first DEL (Panel A) provided two highly enriched (and related) clusters, with the cycle-2 synthon being *p*-tolyl or 3-(trifluoromethyl)phenyl substituted proline, and an amino acid with a 2-methylallyl substitution at cycle-3. There was no preference for building blocks at cycle-1, and the amino acids varied greatly. There is also a strong feature from the second enriched DEL (Panel B). Enriched building blocks in cycle-2 share a similar structural pattern as piperazine substituted benzoic acids. Building blocks at cycle-1 contain varied amino acids, and building blocks at cycle-3 contain aryl rings attached to the cycle-2 building blocks by Suzuki coupling.

We also compared the data performance with that of another reported elution method: heat-on-beads. [39] With the heat-on-beads method, unbound molecules were removed through 5 min heat at 95°C. Molecules bound to target protein immobilized on affinity matrix after the heat elution were directly amplified by PCR on the beads for sequencing. The cubic scatter plot of the heat-on-beads elution method was shown in Fig S1. It was found that in the same covalent libraries, the heat-on-beads elution method did not show clear structural features. It is possible that the on-bead PCR step resulted in higher background signals and lower the signal-to-noise ratio in this case.

On-DNA Compounds Assay

We first re-synthesized the potential hit molecules with their DNA tags attached, employing the same protocols as used in previous library synthesis. [41] These unpurified products were analyzed by LC-MS products and by-products (i.e. truncates) annotated. The product samples were then incubated with SARS-CoV-2 M^{pro} and a gel shift assay was performed to test for covalent binding. The results of this preliminary assay (Fig S2 and Table S2) showed covalent binding of molecules from both hit series to SARS-CoV-2 M^{pro}. With these preliminary results in hand, we proceeded with off-DNA synthesis.

Covalent Binding Assay for Off-DNA Compounds

To validate the covalent binding of the potential hits identified based on our data analysis, we synthesized two series of compounds with different substitutions, including target products and potential by-products. The compound synthesis strategy was to keep the main scaffold of each series and explore the varied building blocks as revealed by the data analysis. For series 1 (Fig. 1A), five different amino acids from building block 1 were selected for 3-(trifluoromethyl)phenyl substituted proline scaffold (**1a-e**) respectively. For series 2 (Fig. 1B), the compounds **2a-b** were synthesized to test if the additional building block at cycle-3 is necessary for activity. Compounds **2c-d** are the full-length compounds with aromatic substitutions at cycle-3. In all cases, the site of the DNA-linker was replaced with methylamide group. The synthetic route and protocol for each compound are provided in the supporting information. All the compound structures are listed in Table. 1.

Intact mass spectrometry (MS) of proteins are widely used in the confirmation of covalent binding and has also been developed as a screening method for fragment-based covalent screening. [26] Therefore, the intact MS of SARS-CoV-2 M^{pro} was analyzed before and after incubation with compounds. Incubations were initially performed with each compound at 100 μM for 1 hr at room temperature, and covalent binding was detected for compounds from both series (Fig. 2A). We then varied incubation times from 1 hr to 24 hrs and observed a time-dependent increasing of labelling percentage. As shown in Fig. 2B, the maximum labelling percentage was reached after 24 hrs incubation, suggesting the relative slow reactivity of the compound **1e** with SARS-CoV-2 M^{pro}.

As an alternative method to prove the covalent binding of compounds with target proteins, we synthesized fluorescent analogs (Cy5 labeled) of compounds **1a** and **2a**. These Cy5 labeled compounds were then incubated with SARS-CoV-2 M^{pro} at 100 μM for 1 hr at room temperature. SDS-PAGE analysis of the resulting mixtures was then performed, and the fluorescent signal of Cy5 was measured and compared with protein bands detected by Coomassie blue staining. The overlap of Cy5 signal and Coomassie blue stained SARS-CoV-2 M^{pro} indicates covalent binding of compounds **1a-Fluo** (compound 1a-Fluorescence) and **2a-Fluo** (compound 2a-Fluorescence) (Fig. 2C). To gain a sense of the selectivity of our molecules, we further investigated the reaction of **1a-Fluo** and **2a-Fluo** with SARS-CoV-2 M^{pro} in the presence of cell lysate, where the strongest Cy5 signal still overlapped with Coomassie blue stained SARS-CoV-2 M^{pro} (Fig. 2**D**). These results suggest our hit compounds are moderately selective for SARS-CoV-2 M^{pro}.

Table 1
Structures of off-DNA resynthesized compounds from two series.

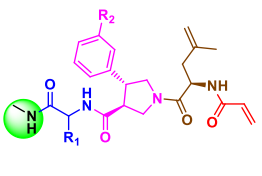

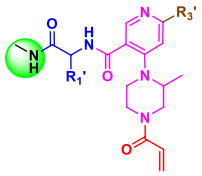

Compound #	R_1	R_2	Compound #	R_1'	R_3'
1a		—CF_3	**2a**		—H
1b		—CF_3	**2b**		—Cl
1c		—CF_3	**2c**		
1d		—CF_3	**2d**		
1e		—CF_3			

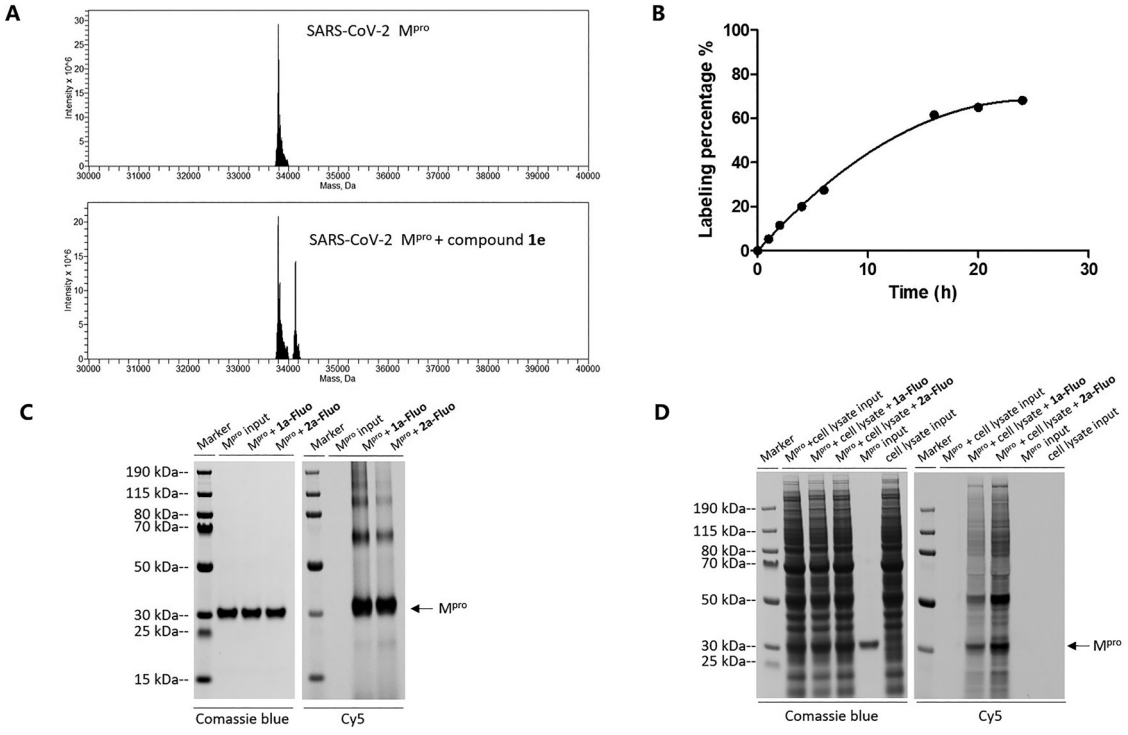

Figure 2. The covalent binding of hit compounds as determined by LC-MS and fluorescent staining assay. (**A**) Representative protein intact MS of hit compound covalently binding with SARS-CoV-2 M^{pro}. (**B**) Time-dependent increasing of the labeling percentage for compound **1e** as determined by LC-MS. (**C**) Fluorescent analogs (Cy5 labeled) of compounds **1a** and **2a** were synthesized and incubated with **SARS-CoV-2 Mpro. SDS-PAGE analysis of the resulting mixtures was then performed and the** Cy5 signal which overlaps with the protein bands (Coomassie blue) suggested the formation of covalent complex between protein and hit compounds. **1a-Fluo** and **2a-Fluo** represent compound 1a- and 2a-Fluorescence respectively. (**D**) Similar fluorescent staining assay as in 2C was performed for covalent binding in the presence of cell lysate. The Cy5 signal which is mainly corresponding to the target protein bands (Coomassie blue) suggested the formation of covalent complex between protein and hit compounds.

Table 2
Summary of the enzymatic activity and inhibitory activity against SARS-CoV-2 infection.

Compound #	SARS-2[a] IC50 (μM)	SARS-1[a] IC50 (μM)	OC43[a] IC50 (μM)	MERS[a] IC50 (μM)	229E[a] IC50 (μM)	HKU1[a] IC50 (μM)	NL63[a] IC50 (μM)
1a	>100	>100	>100	>100	>100	>100	>100
1b	22.8	47.8	>100	>100	>100	>100	>100
1c	61.6	61.7	>100	>100	>100	>100	>100
1d	>100	>100	>100	>100	>100	>100	>100
1e	2.0	3.5	37.4	>100	1.8	19.5	>100
2a	36.5	74.2	45.9	>100	>100	52.2	>100
2b	51.0	93.1	66.6	>100	>100	80.1	>100
2c	>100	>100	>100	>100	>100	>100	>100
2d	>100	>100	>100	>100	>100	>100	>100
GC376	0.013	0.026	0.014	0.153	0.026	0.012	0.052

[a] The IC_{50} value as determined by the enzymatic assays of the corresponding main protease. The values were calculated from ten data points with two independent determinations.

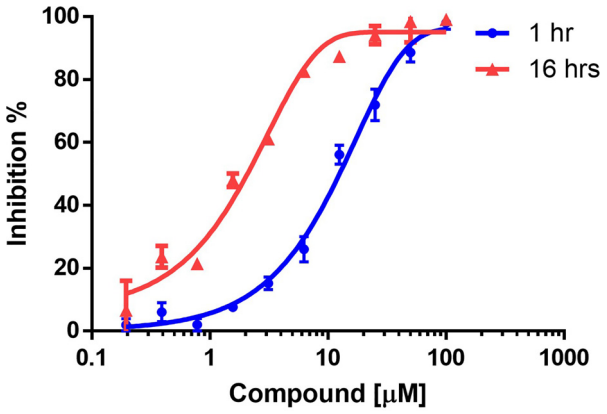

Figure 3. Time-dependent enzymatic assay of compound **1e** for SARS-CoV-2 main protease. The IC_{50} value with 1 hr and 16 hrs incubation time were 15.9 μM and 1.9 μM respectively. The values were calculated from ten data points with three independent determinations.

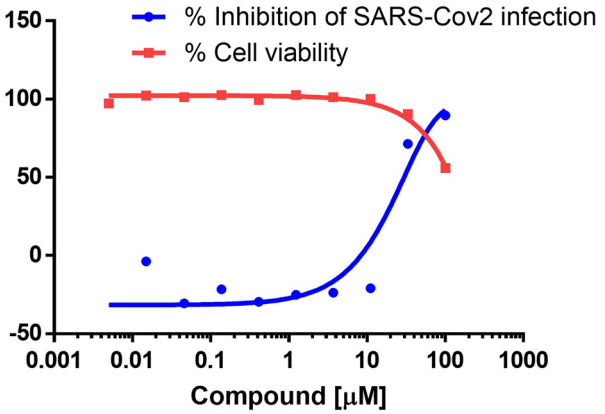

Figure 4. The inhibition of SARS-CoV-2 infection and the effect on cell viability of compound **1e**. The antiviral EC_{50} value was 33 μM, CC_{50} value was more than 100 μM. The values were calculated from ten data points with two independent determinations, using 2 uM CP-100356 only group as a control for 0% inhibition.

Enzymatic activity assay

Next, we investigated the inhibitory effect of our hit molecules against the main protease of different coronaviruses including SARS-2, SARS-1, OC43, MERS, 229E, HKU1 and NL63 CoV. [15] The results are summarized in Table 2. Compound **1a-b** appears to be the most potent overall, and compound **1e** possess the lowest IC_{50} value against SARS-CoV-2 M^{pro}. Compound **1e** also showed the highest covalent binding percentage as judged by LC-MS, suggesting that enzymatic inhibition results from covalent binding. It is not surprising that these compounds show activity against main proteases of other coronaviruses, especially for SARS-CoV-1. The main proteases in different genera possess sequence identity close to 50%, along with high tertiary and quaternary structural conservation especially in the region around the main pocket. [43] Moreover, we tested the inhibitory effect of our hit compound **1e** against the main protease of SARS-CoV-2 at 1 hr and 16 hrs. The results showed that as the incubation time increases, the IC_{50} decreases (Fig. 3), which is consistent with the time-dependent nature of covalent reaction.

SARS-CoV-2 Antiviral Assay

We wonder if these compounds are functionally active in the cellular assay of SARS-CoV-2 infection. With reference to the reported strategy on antiviral assays in co-dosing P-glycoprotein transport inhibitor to reduce cellular efflux, the cell was treated with compound **1e** ten-point dose from 100 μM in the presence of 2 μM CP-100356, which is a known P-glycoprotein transport inhibitor to suppress the high efflux potential of the assay cell line. [44] As shown in Fig. 4, compound **1e** showed inhibitory effect against SARS-CoV-2 infection by the cellular assay. The 50% effective concentration (EC_{50}) was around 33 μM while it was found with moderate cytotoxic activity up from 100 μM. The cytotoxicity and relative higher EC_{50} in cell-based assay might be arise from the off-target effects previously identified from gel shift assay in the presence of cell lysate. Further optimization work is needed to address this problem to achieve higher potency and selectivity.

Molecular Modelling

In an effort to understand the key interactions between SARS-CoV-2 M^{pro} and the covalent binders, we performed covalent docking on **1e** and **2a**. [45] Our docking results showed that both **1e** and **2a** formed hydrogen bonds with Gly143 in the active site (Fig. 5). However, their binding modes were significantly different. In compound **1e**, the 3-(trifluoromethyl)phenyl group was accommodated in the S4 subpocket consisting of Met165, Leu167, Phe185, Gln189, and Gln192. [46, 47] Meanwhile, the R_1 moiety at cycle one, a benzyl group in **1e**, was fit into another subsite S1 comprising of Phe140, Asn142, His163, Glu166, and His172, which might explain the weaker binding affinities of **1a** and **1d** in this series, as the proper size and the aromaticity of the R_1 group seem to be important (Fig. 5**A**). A hydrogen bond was also formed between the terminal methylamide group and Glu166. For compound **2a**, a plausible binding mode was observed and shown in Fig. 5**B**. The R_1' group of **2a** was near the S4 pocket, but did not extend into it. Furthermore, the significantly reduced binding affinity of **2c** and **2d** may be caused by the steric hindrance between the non-hydrogen moieties of R_3'group and Thr25 in the vicinity. The methylamide group at cycle-1 for both **1e** and **2a** was found to at the edge of the binding pocket,

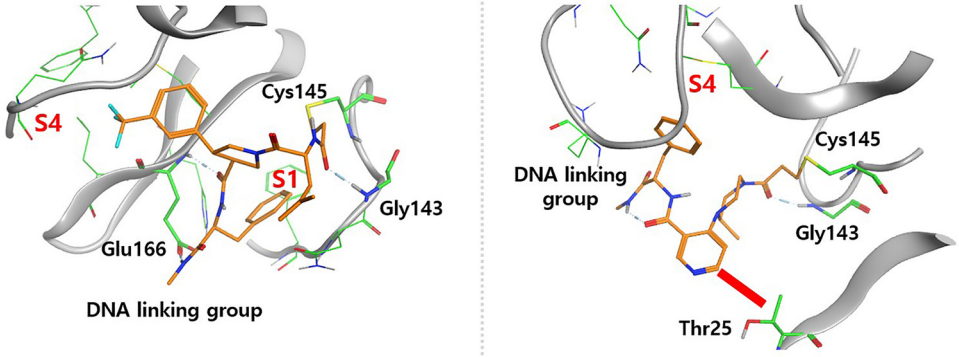

Figure 5. The covalent docking poses of compounds (**A**) **1e** and (**B**) **2a**. Orange and green: carbon; Blue: nitrogen; Red: oxygen; Yellow: sulfur; Cyan: fluorine. The red bar in (**B**) indicates the potential steric hindrance when R_3' is a heavy atom or a functional group.

which allows for the exit of the DNA tag. These results shed insight on the further hit-to-lead optimization to develop compounds with better activity.

To date, the main challenge in developing novel covalent inhibitors is a lack of chemically diverse compound collections available for high-throughput screening. To circumvent this problem, drug hunters often focus on the addition of electrophiles to known non-covalent binders using rational design techniques. However, this strategy has disadvantages including long time-lines and a lack of chemical starting points. [48] Herein we demonstrate the use of DNA-encoded libraries to directly discover covalent hit molecules against the protease SARS-CoV-2 M^{pro}, complementing recently published work targeting a kinase using similar techniques for library production and selection. [40] Two novel covalent hit series against SARS-CoV-2 M^{pro} were discovered. These hit molecules bind SARS-CoV-2 M^{pro} covalently in a 1:1 stoichiometry. Enzymatic activity against a panel of main proteases was determined, and the most potent molecule (**1e**) shows activity against 6 of the 8 main protease homologs. The most potent compound also showed inhibitory effect against SARS-CoV-2 in cellular assay. Lastly, the binding model of our hit molecules with the main pocket of SARS-CoV-2 M^{pro} was analyzed by the molecular modelling, and further optimization appears possible.

Supplemental material

Supplemental_Material_for_Discovery_of_SARS-CoV-2_Main_Protease_Covalent_Inhibitors_from_a_DNA-Encoded_Library_Screening_by_Wenji,_et_al.pdf

Supplemental material is available online with this article. Including experimental details of the preparation and characterization of all target compounds, experimental procedure and supporting figures.

Funding

The authors received no financial support for the research, authorship, and/or publication of this article.

Author contributions

Rui Ge: covalent DEL selection, experiment design, and manuscript preparation. Zuyuan Shen: project tracking, off-DNA compounds preparation, figure preparation and manuscript preparation. Jian Yin: molecular modelling, figure preparation, and manuscript preparation. Wenhua Chen: DEL selection data analysis. Qi Zhang and Yulong An: covalent DEL construction. Dewei Tang and Alexander L. Satz: manuscript proofreading and editing. Wenji Su: overall study design, manuscript proofreading and editing. Letian Kuai: overall study design, manuscript proofreading and editing.

Declaration of Conflicting Interests

The authors declared the following potential conflicts of interest with respect to the research, authorship, and/or publication of this article: All authors were employed by WuXi AppTec, and their research and authorship of this article was completed within the scope of their employment with WuXi AppTec.

Acknowledgments

We are grateful to Dr. Yue Li, Shunjie Pan, Jing He and Youlang Yuan for expert opinion and support of this work. We would like to thank the CSU team in WuXi AppTec for assistance in synthesis of off-DNA compounds. We also thank coronavirus platform in WuXi biology for assistance in enzymatic activity assay.

Supplementary materials

Supplementary material associated with this article can be found, in the online version, at doi:10.1016/j.slasd.2022.01.001.

References

[1] Paules CI, Marston HD, Fauci AS. Coronavirus Infections-More than Just the Common Cold. JAMA 2020;323:707–8.
[2] Dhama K, Khan S, Tiwari R, et al. Coronavirus disease 2019-COVID-19. Clin Microbiol Rev 2020;33 e00028-20.
[3] Zhao J, Zhao S, Ou J, et al. COVID-19: Coronavirus vaccine development updates. Frontiers in immunology 2020;11:602256–7.
[4] Rabaan AA, Al-Ahmed SH, Sah R, et al. SARS-CoV-2/COVID-19 and advances in developing potential therapeutics and vaccines to counter this emerging pandemic. Ann Clin Microbiol Antimicrob 2020;19:40.
[5] Li YD, Chi WY, Su JH, et al. Coronavirus vaccine development: from SARS and MERS to COVID-19. J Biomed Sci 2020;27:104.
[6] Harrison C. Coronavirus puts drug repurposing on the fast track. Nat Biotechnol 2020;38:379–81.
[7] Asselah T, Durantel D, Pasmant E, et al. COVID-19: Discovery, diagnostics and drug development. J Hepatol 2021;74:168–84.
[8] Ghosh AK, Brindisi M, Shahabi D, et al. Drug development and medicinal chemistry efforts toward SARS-coronavirus and covid-19 therapeutics. ChemMedChem 2020;15:907–32.
[9] Khare P, Sahu U, Pandey SC, et al. Current approaches for target-specific drug discovery using natural compounds against SARS-CoV-2 infection. Virus Res 2020;290:198169.
[10] Riva L, Yuan S, Yin X, et al. Discovery of SARS-CoV-2 antiviral drugs through large-scale compound repurposing. Nature 2020;586:113–19.
[11] Zhou Y, Wang F, Tang J, et al. Artificial intelligence in COVID-19 drug repurposing. Lancet Digit Health 2020;2:e667–76.
[12] Ullrich S, Nitsche C. The SARS-CoV-2 main protease as drug target. Bioorg Med Chem Lett 2020;30:127377.
[13] Wang YC, Yang WH, Yang CS, et al. Structural basis of SARS-CoV-2 main protease inhibition by a broad-spectrum anti-coronaviral drug. Am J Cancer Res 2020;10:2535–45.
[14] Wang MY, Zhao R, Gao LJ, et al. SARS-CoV-2: Structure, biology, and structure-based therapeutics development. Front Cell Infect Microbiol 2020;10:587269.
[15] Jin Z, Du X, Xu Y, et al. Structure of M(pro) from SARS-CoV-2 and discovery of its inhibitors. Nature 2020;582:289–93.
[16] Dai W, Zhang B, Jiang XM, et al. Structure-based design of antiviral drug candidates targeting the SARS-CoV-2 main protease. Science 2020;368:1331–5.

[17] Banerjee R, Perera L, Tillekeratne LMV. Potential SARS-CoV-2 main protease inhibitors. Drug Discov Today 2021;26:804–16.
[18] Badua C, Baldo KAT, Medina PMB. Genomic and proteomic mutation landscapes of SARS-CoV-2. J Med Virol 2021;93:1702–21.
[19] Sutanto F, Konstantinidou M, Domling A. Covalent inhibitors: a rational approach to drug discovery. RSC Med Chem 2020;11:876–84.
[20] Ghosh AK, Samanta I, Mondal A, et al. Covalent inhibition in drug discovery. ChemMedChem 2019;14:889–906.
[21] De Cesco S, Kurian J, Dufresne C, et al. Covalent inhibitors design and discovery. Eur J Med Chem 2017;138:96–114.
[22] Dalton SE, Campos S. Covalent small molecules as enabling platforms for drug discovery. Chembiochem 2020;21:1080–100.
[23] Gehringer M, Laufer SA. Emerging and re-emerging warheads for targeted covalent inhibitors: Applications in medicinal chemistry and chemical biology. J Med Chem 2019;62:5673–724.
[24] Lonsdale R, Ward RA. Structure-based design of targeted covalent inhibitors. Chem Soc Rev 2018;47:3816–30.
[25] Keeley A, Petri L, Abranyi-Balogh P, et al. Covalent fragment libraries in drug discovery. Drug Discov Today 2020;25:983–96.
[26] Resnick E, Bradley A, Gan J, et al. Rapid covalent-probe discovery by electrophile-fragment screening. J Am Chem Soc 2019;141:8951–68.
[27] Goodnow RA Jr, Dumelin CE, Keefe AD. DNA-encoded chemistry: enabling the deeper sampling of chemical space. Nat Rev Drug Discov 2017;16:131–47.
[28] Satz AL, Kuai L, Peng X. Selections and screenings of DNA-encoded chemical libraries against enzyme and cellular targets. Bioorg Med Chem Lett 2021;39:127851.
[29] Favalli N, Bassi G, Scheuermann J, et al. DNA-encoded chemical libraries - achievements and remaining challenges. FEBS Lett 2018;592:2168–80.
[30] Song M, Hwang GT. DNA-encoded library screening as core platform technology in drug discovery: Its synthetic method development and applications in DEL synthesis. J Med Chem 2020;63:6578–99.
[31] Madsen D, Azevedo C, Micco I, et al. An overview of DNA-encoded libraries: A versatile tool for drug discovery. Prog Med Chem 2020;59:181–249.
[32] Ottl J, Leder L, Schaefer JV, et al. Encoded library technologies as integrated lead finding platforms for drug discovery. Molecules 2019;24:1629.
[33] Zhao G, Huang Y, Zhou Y, et al. Future challenges with DNA-encoded chemical libraries in the drug discovery domain. Expert Opin Drug Discov 2019;14:735–53.
[34] Cochrane WG, Malone ML, Dang VQ, et al. Activity-based DNA-encoded library screening. ACS Comb Sci 2019;21:425–35.
[35] Kodadek T, Paciaroni NG, Balzarini M, et al. Beyond protein binding: recent advances in screening DNA-encoded libraries. Chem Commun (Camb) 2019;55:13330–41.
[36] Chan AI, McGregor LM, Jain T, et al. Discovery of a covalent kinase inhibitor from a DNA-encoded small-molecule library x protein library selection. J Am Chem Soc 2017;139:10192–5.
[37] Zimmermann G, Rieder U, Bajic D, et al. A specific and covalent JNK-1 ligand selected from an encoded self-assembling chemical library. Chemistry 2017;23:8152–5.
[38] Zambaldo C, Daguer JP, Saarbach J, et al. Screening for covalent inhibitors using DNA-display of small molecule libraries functionalized with cysteine reactive moieties. Med. Chem. Commun. 2016;7:1340–51.
[39] Zhu Z, Grady LC, Ding Y, et al. Development of a selection method for discovering irreversible (Covalent) binders from a DNA-encoded library. SLAS Discov 2019;24:169–74.
[40] John PG, Archna A, Martin A, et al. Novel irreversible covalent BTK inhibitors discovered using DNA-encoded chemistry. Bioorg. Med. Chem. 2021;42:116223.
[41] Kuai L, O'Keeffe T, Arico-Muendel C. Randomness in DNA encoded library selection data can be modeled for more reliable enrichment calculation. SLAS Discov 2018;23:405–16.
[42] Su W, Ge R, Ding D, et al. Triaging of DNA-encoded library selection results by high-throughput resynthesis of DNA-conjugate and affinity selection mass spectrometry. Bioconjug Chem 2021;32:1001–7.
[43] Roe MK, Junod NA, Young AR, et al. Targeting novel structural and functional features of coronavirus protease nsp5 (3CL pro, M pro) in the age of COVID-19. J Gen Virol 2020;102:001558.
[44] Hoffman RL, Kania RS, Brothers MA, et al. Discovery of Ketone-Based Covalent Inhibitors of Coronavirus 3CL Proteases for the Potential Therapeutic Treatment of COVID-19. J Med Chem 2020;63:12725–47.
[45] Molecular Operating Environment (MOE) Chemical Computing Group ULC 201901, Montreal, QC, Canada: 1010 Sherbooke St West, Suite #910; 2021. H3A 2R7.
[46] doi:10.1126/science.abb3405.
[47] https://doi.org/10.3389/fmolb.2020.599079.
[48] Hansen R, Peters U, Babbar A, et al. The reactivity-driven biochemical mechanism of covalent KRAS(G12C) inhibitors. Nat Struct Mol Biol 2018;25:454–62.